ELSEVIER

PII:S0958-9465(98)00004-3

Cement and Concrete Composites **20** (1998) 353–363
0958-9465/98/$ — see front matter

Fatigue Characteristics of High Performance Fiber-reinforced Concrete

A. E. Naaman* & H. Hammoud

Department of Civil and Environmental Engineering, University of Michigan, Ann Arbor, MI 48109-2125, USA

Abstract

This paper provides a summary of a study on fatigue behavior undertaken as part of SHRP project C-205 on the fresh and hardened properties of high early strength fiber-reinforced concrete (HESFRC). HESFRC was defined as achieving a minimum target compressive strength of 5 ksi (35 MPa) in 24 h. Several properties of HESFRC were investigated: for the fresh mixture, the air content, inverted slump test, temperature, and unit weight; for the hardened composite, the compressive, bending, and tensile properties. Optimum mixtures that satisfied the minimum compressive strength criterion, and showed excellent values of modulus of rupture, toughness indices in bending, and split tensile behavior, were selected for fatigue testing. In this paper a description is given of key results of the fatigue bending tests only.

The experimental program included a total of 24 fiber-reinforced concrete flexural specimens, ten of which were control specimens tested under static flexural loading, and the remaining 14 specimens were tested under fatigue loading. Two mixes containing 2 vol% of hooked steel fibers were selected. For each mix, three different target load ranges were applied: 10–70%, 10–80%, and 10–90% of the ultimate flexural capacity, as obtained from the corresponding control static test with fibers. A typical relation between maximum fatigue stress and number of cycles to failure was derived, suggesting a fatigue endurance limit of the order of 65% even if specimens are in a cracked state. © 1998 Elsevier Science Ltd. All rights reserved.

Keywords: fatigue, fiber-reinforced concrete.

INTRODUCTION

The study described in this paper was part of a project sponsored by the Strategic Highway Research Program (SHRP). SHRP project C-205 dealt with the mechanical properties of high performance concretes; it was completed in 1993 with research findings compiled in six volumes, the sixth volume being devoted to the fresh and mechanical properties of high early strength fiber-reinforced concrete (HESFRC).[1,2]

The main objectives of the experimental study for HESFRC were to: (1) establish a consistent and comprehensive data base on HESFRC; (2) document and synthesize information on the properties of the fresh mixture and the mechanical properties of the hardened composite; (3) draw some practical recommendations for use of HESFRC by the profession. It should be noted that, although several thousand investigations have dealt with fiber-reinforced concrete, none comprises the overall range of tests (from the fresh state to the hardened composite) and the overall range of parameters, and none provides the same consistent testing procedures throughout, as undertaken in this study. This experimental investigation has followed an initial evaluation

*To whom correspondence should be addressed.

of existing knowledge in the field which was summarized in an earlier state-of-the-art report[3] and an annotated bibliography on high performance fiber-reinforced concrete.[4]

Definition — scope

As with high early strength (HES) concrete, HESFRC was defined as achieving a minimum target compressive strength of 5 ksi (35 MPa) in 24 h. Since the minimum strength criterion could be satisfied with the control specimens without fibers, and since in current applications of fiber-reinforced concrete for pavements, only low fiber contents (0.10 to 1 vol% of concrete) are used, it was decided to explore and document a higher range of fiber content (1 and 2 vol% of concrete). The main intent was to achieve, in addition to the minimum specified target compressive strength, a post-cracking strength in bending (i.e. a modulus of rupture) higher than the cracking strength so as to minimize crack widths and insure a sufficient resistance to repeated loads after cracking. This is typically a characteristic of high performance fiber-reinforced cement composites.[5] It led to a load–deflection response with a post-cracking resistance above the cracking load level, at deflections up to five times the deflection at cracking. It implied a minimum ductility behavior in bending otherwise not present in the control specimens without fibers or with very small fiber contents.

Fresh HESFRC properties included air content, inverted slump test, temperature, and plastic unit weight. Tests on the mechanical properties included compressive strength, elastic modulus, flexural strength, splitting tensile strength, and fatigue life. Seventeen different combinations of parameters were investigated for each type of test. The main parameters included: (1) three different matrix mixtures (one control, one with silica fume and one with latex); (2) two different volume fractions of fibers (1 and 2%); (3) two fiber materials (steel and polypropylene); (4) two steel fiber lengths, corresponding to aspect ratios of 60 and 100; (5) hybrid mixes containing either an equal amount of steel and polypropylene fibers, or an equal amount of steel fibers of different lengths. The compression and the bending tests also included a time variable, i.e. they were measured at ages 1, 3, 7, and 28 days. Information from the compression tests comprised the compressive strength, the elastic modulus, and the strain capacity. Optimum mixtures that satisfied the minimum compressive strength criterion, and showed excellent values of modulus of rupture, toughness indices in bending, and split tensile behavior, were selected for fatigue testing. Here, only that part of the study dealing with fatigue is described.

Details, as well as references to several studies or documents used to gather information or develop technical background during this investigation, are given in Refs [1–4,6–8].

EXPERIMENTAL PROGRAM FOR FATIGUE

An experimental program was carried out to investigate the effects of repetitive flexural fatigue loading on HESFRC. Details are given in Ref. 1. A total of 24 fiber-reinforced concrete flexural specimens were tested, ten of which were control specimens tested under static flexural loading, and the remaining 14 specimens were tested under fatigue loading. Two mixes containing 2 vol% of hooked steel fibers were selected. The first mix used the Dramix 30/50 (length 30 mm; diameter 0.5 mm; aspect ratio 60) fibers, whereas the second mix (hybrid mix) used an equal amount of Dramix 30/50 and Dramix 50/50 (length 50 mm; diameter 0.5 mm; aspect ratio 100) fibers. The composition of the matrix, for the control as well as the fiber-reinforced mixture, was as follows: type III cement; water to cement ratio 0.34; sand to cement ratio 1.47; coarse aggregate to cement ratio 1.82; superplasticizer to cement ratio up to 0.035; corrosion inhibitor to cement ratio 0.092. Prior tests under the same program gave the following results for the average compressive strength at 28 days obtained from 4×8 in^2 (100×200 mm^2) cylinders: 7 ksi (48.3 MPa) for the control mix without fibers; 7.6 ksi (52.4 MPa) for the mix with 2% Dramix 30/50 steel fibers; 6.91 ksi (47.7 MPa) for the hybrid mix with the combination of Dramix 30/50 and 50/50 steel fibers. The slight drop in strength for the hybrid mix was attributed to the additional air entrained because of the difficulty in mixing longer fibers. The flexural specimens were 16 in (400 mm) long with a square cross-section of 4×4 in^2 (100×100 mm^2). They were tested in third-point loading at a clear span of 12 in (300 mm) according to ASTM C 1018. The age at testing exceeded 60 days.

For each mix, three different target load ranges were applied: 10–70%, 10–80%, and 10–90% of the ultimate flexural capacity, as obtained from the corresponding control static test with fibers.

TEST PROCEDURE

All flexural tests were performed in a servo-controlled MTS hydraulic testing machine, Model 810. Three types of measurement were recorded for each beam: (1) the load from the load cell of the testing machine; (2) the vertical deflection at the third points; (3) the bottom tensile elongation measured over a 4 in (10 cm) gage length between the load application points. The vertical deflection was measured by two LVDTs placed at the third points on opposite sides of the test beam. The bottom tensile elongation (also described as strain capacity) was obtained by one LVDT placed under the specimen along its plane of symmetry and attached to a special aluminum frame, which in turn was fixed to the specimen third points. All measurements were recorded via a computerized data acquisition system. Some details of the test set-up are shown in Figs 1 and 2.

Before fatigue testing, all specimens were subjected to a non-destructive test to determine their dynamic elastic modulus. The resonant frequency method (ASTM C 215-60) was used. The prismatic specimens were subjected to flexural vibration, and the resonance frequencies of the fundamental mode were recorded. These values were then used to determine the dynamic modulus according to the expression provided in the standard. Values of dynamic modulus for all specimens tested are summarized in Table 1. It was assumed that such values may provide an additional measure of the prediction of the strength of the fatigue specimen, and thus a possible correlation with the cyclic behavior observed.

The control static flexural tests were performed under displacement control. Measurements of the load, deflections at the third points, and tensile elongation at the bottom fiber were recorded, and the ultimate flexural capacity (MOR) was obtained (Tables 1 and 2). All static test results of specimens with the 30 mm long fibers had normal scatter, i.e. within the range observed in the bending test program undertaken separately.[7] A relatively large scatter in the static test results was observed for the hybrid specimens containing a mix of 30 mm and 50 mm long fibers (Table 1). This could be attributed to the poorer uniformity of mixing of the longer fibers and the relatively large size of the fiber (50 mm) to the specimen minimum dimension (100 mm).

The fatigue tests were performed under load control. Each specimen was first subjected to three slow cycles between the minimum and maximum load, to record the initial hysteresis loops and stabilize the specimen. Then the specimen was subjected to a sinusoidal wave cyclic fatigue loading with a frequency that,

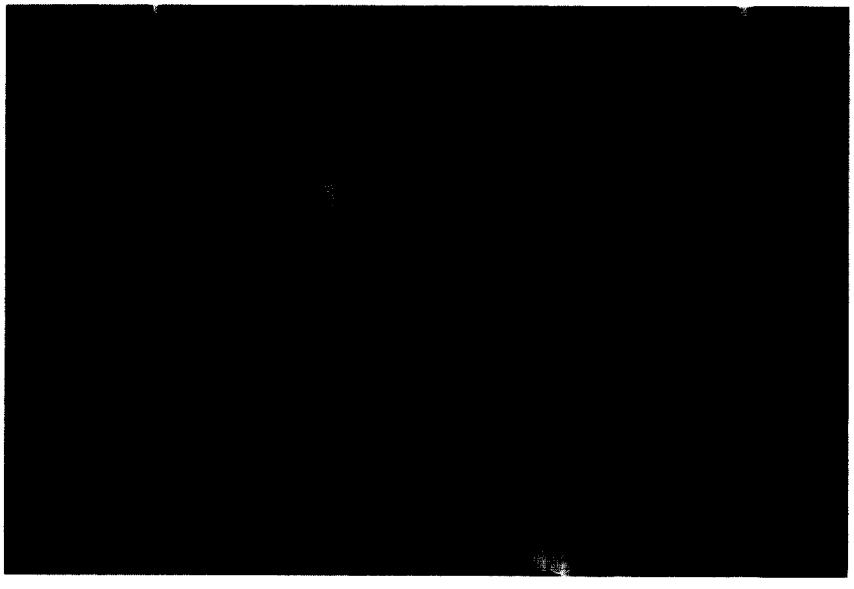

Fig. 1. Photograph of instrumented specimen.

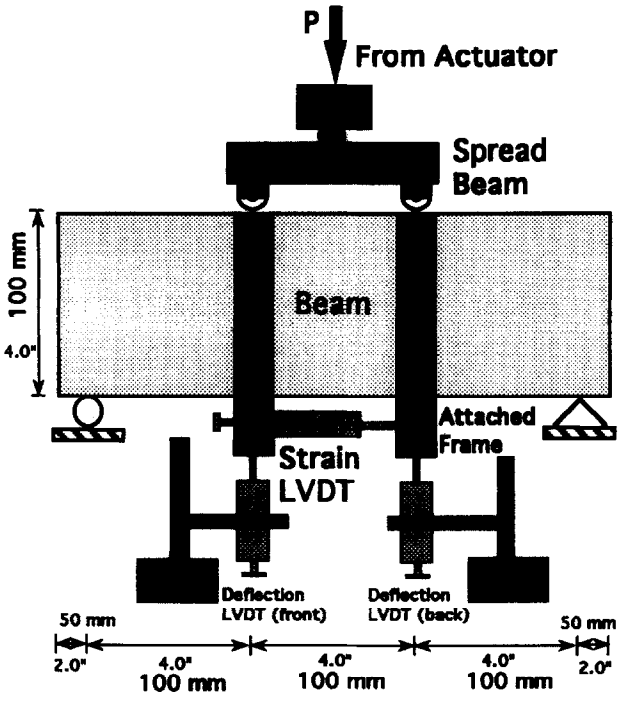

Fig. 2. Specimen dimensions and special measuring devices.

depending on the load range and expected fatigue life, varied between 1 and 5 Hz. The fatigue test was interrupted periodically at a selected number of cycles to record, at a slow rate, an entire hysteresis loop between the minimum and the maximum load. The hysteresis loops were obtained for the load versus average third-point deflection and the load versus tensile elongation (or equivalently the strain capacity) at the bottom fiber. Only two to three specimens were tested under every loading range. The specimens were subjected to a constant load range fatigue loading until failure or 5×10^6 cycles, whichever occurred first. The two specimens that survived 5×10^6 cycles were then subjected to a static bending test up to failure.

It should be noted that all specimens tested in this study were precracked before cyclic loading, with two to three visible cracks in the constant moment region. This is an essential characteristic of these tests compared with previous studies on fatigue of fiber-reinforced concrete, such as those by Batson *et al.*[9], Ramakrishnan and coworkers[10–12] and Wei *et al.*[13] which are further described below.

Figure 3 shows a photograph of a typical specimen that failed under fatigue loading. As observed for all specimens, one major crack (out of two to three visible ones) propagated in the constant moment region until final failure of the specimen occurred.

Table 1. Results of dynamic modulus and modulus of rupture tests

Specimen no.	*Batch no.*	*Mix ID (Vf = 2%)*	*Dynamic modulus E_{dyn} (ksi (GPa))*	*Type of test*	*Static modulus of rupture MOR (psi (MPa))*
0	—	—	— [a]	Static	790 (5.45)
1	I	A2%S3	— [a]	Static	1382 (9.55)
2	I	A2%S3	4210 (29)	Fatigue	NA
3	I	A2%S3	4203 (29)	Static	1266 (8.73)
4	II	A2%S3	4221 (29.1)	Fatigue	NA
5	II	A2%S3	4398 (30.3)	Fatigue	NA
6	II	A2%S3	4249 (29.3)	Static	1346 (9.29)
7	III	A2%S3	4846 (33.4)	Static	1408 (9.71)
8	III	A2%S3	4961 (34.2)	Fatigue	NA
9	III	A2%S3	5421 (37.4)	Fatigue	NA
10	IV	A2%S3	4881 (33.7)	Fatigue	NA
11	IV	A2%S3	4777 (33)	Static	1722 (11.88)
12	IV	A2%S3	4768 (32.9)	Fatigue	NA
13	III	A2%S3S5	4799 (33.1)	Static	1371 (9.46)
14	III	A2%S3S5	— [a]	Static	1807 (12.47)
15	III	A2%S3S5	3993 (27.6)	Fatigue	NA
16	IV	A2%S3S5	4573 (31.6)	Fatigue	NA
17	IV	A2%S3S5	4870 (33.6)	Fatigue	NA
18	IV	A2%S3S5	5189 (35.8)	Fatigue	NA
19	I	A2%S3S5	5090 (35.1)	Static	2187 (15.09)
20	I	A2%S3S5	4090 (28.2)	Fatigue	NA
21	I	A2%S3S5	5140 (35.5)	Fatigue	NA
22	II	A2%S3S5	5355 (36.9)	Static	3000 (20.7)
23	II	A2%S3S5	4973 (34.3)	Static	2190 (15.11)
24	II	A2%S3S5	5475 (37.8)	Fatigue	NA

[a] No test was undertaken.

Table 2. Results of fatigue tests

Specimen no.	*Mix ID (Vf = 2%)*	*Reference static MOR (psi (MPa))*	*Target load range (%)*	*Cycles to failure N_f*	*Corrected load range (%)*	*MOR after cycling (psi (MPa))*
2	A2%S3	1312 (9.05)	10–80	3679	—	—
4	A2%S3	1294 (8.93)	10–90	9	—	—
5	A2%S3	1294 (8.93)	10–80	3900	—	—
8	A2%S3	1406 (9.70)	10–70	2881222	—	—
9	A2%S3	1406 (9.70)	10–70	5276028[a]	7.5–52	1875 (12.94)
10	A2%S3	1687 (11.64)	10–70	108195	—	—
12	A2%S3	1687 (11.64)	10–90	23	—	—
15	A2%S3S5	1800 (12.42)	10–90	2	—	—
16	A2%S3S5	1800 (12.42)	10–90	4	—	—
17	A2%S3S5	1800 (12.42)	10–70	5000000[a]	7.1–57	2531 (17.46)
18	A2%S3S5	2175 (15)	10–70	1910942	—	—
20	A2%S3S5	2175 (15)	10–80	15000	—	—
21	A2%S3S5	2175 (15)	10–80	8964	—	—
24	A2%S3S5	2175 (15)	10–70	1440058	—	—

[a] Specimen did not fail under fatigue loading but was loaded monotonically to failure after cycling.

DATA ANALYSIS AND TEST RESULTS

Monotonic tests were undertaken first to establish reference values. The static value of modulus of rupture, MOR, ranged from 1294 to 2175 psi (9 to 15 MPa) for a compressive strength range of 6.91 to 7.60 ksi (48 to 53 MPa). The MOR of the control concrete without fibers was 790 psi (5.5 MPa), and its compressive strength was 7 ksi (49 MPa). The average MOR value from the static tests with 2% fibers was 1728 psi (12 MPa). As the modulus of rupture was higher than the cracking strength, and because the concrete mixes tested exhibited multiple cracking behavior, they can qualify as high performance fiber-reinforced concrete composites.

The reference MOR (or flexural strength) used to adjust fatigue load ranges for a given specimen was taken as that of the sister specimen of the same mix with fibers tested under static loading at the same time as the fatigue test (Table 2).

The data recorded from the fatigue experiments were plotted in several ways, which include load versus deflection curves and load versus strain capacity curves under both static or cyclic loading, and increases in deflection or strain capacity with the number of cycles of loading. Typical load deflection curves at

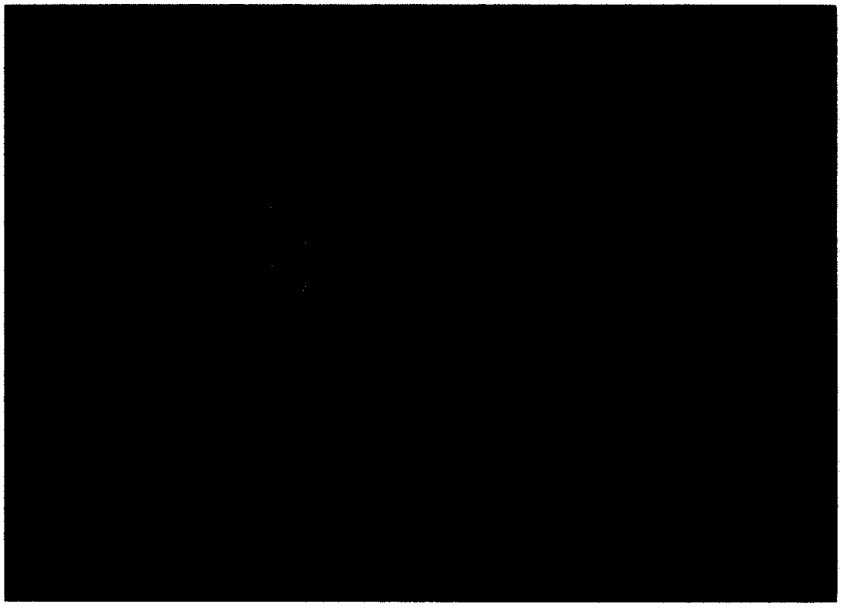

Fig. 3. Typical photograph of specimen failure by fatigue.

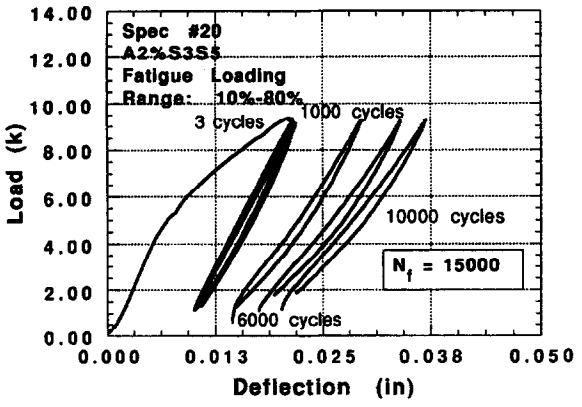

Fig. 4. Load versus deflection hysteretic response of specimen 20 under fatigue loading.

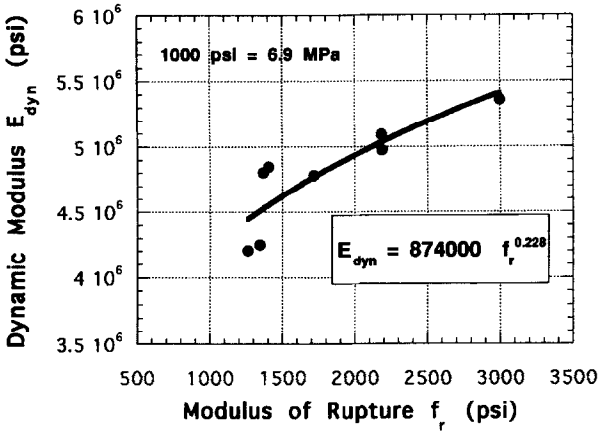

Fig. 5. Modulus of rupture versus dynamic modulus (1 kip = 4448 N; 1 in = 25 mm).

various cycles for one specimen are shown in Fig. 4. Failure occurred by fiber pull-out, when one major crack in the constant moment region propagated toward the compression zone.

The main highlights of the results are described next.

Dynamic modulus of elasticity

The main reason for running the dynamic modulus tests was to provide some correlation between the MOR and the dynamic modulus, thus allowing for an additional method to predict the MOR of the fatigue specimen. This should provide a means to introduce a possible correction in the cyclic load range applied or to better explain certain results with large variability.

A comparison between the flexural strength (MOR) and the dynamic modulus data was carried out for the specimens tested under static loading. The trend observed is illustrated in Fig. 5. A power curve was fitted, leading to the following relation between the dynamic modulus E_{dyn} and the MOR f_r:

$$E_{dyn} = 874\,000 f_r^{0.228} \text{ (psi)} \quad (1a)$$

$$E_{dyn} = 18\,800 f_r^{0.228} \text{ (MPa)} \quad (1b)$$

with a coefficient of correlation of 0.85. The correlation was not considered sufficient to recommend proceeding on that basis.

Table 1 gives the values of the dynamic modulus of the specimens tested, and Table 2 gives their fatigue life. It should be observed that a high value of dynamic modulus (specimens 9, 18, 21, 24) does not necessarily correspond to a high value of fatigue life for the range of loading used, here also implying a poor correlation between them.

Fatigue life and endurance limit

The fatigue life of a specimen is defined as the number of cycles to failure at the given loading range. A large scatter is usually observed in fatigue life, even in the most carefully planned tests. This is because a small error in the estimate of the ultimate strength induces an error in the load range, which in turn can have an enormous effect on the number of cycles to failure.

Owing to the limited scope of this study, only two to three specimens were tested under every loading range. Results are presented in Table 2. In the table, the target load ranges based on the flexural strength of the control test are shown in percent.

It can be observed from Table 2 that the specimens subjected to a loading range between 10 and 90% of the ultimate strength had a very low fatigue life. A major crack was always observed in the first cycle, and with further cycling it would propagate rapidly towards the compression zone of the specimen, leading to its final collapse. The two specimens of series A2%S3 sustained 9 and 23 cycles, and the two specimens of series A2%S3S5 sustained only 2 and 4 cycles to failure.

The specimens subjected to the 10 to 80% loading range sustained the following numbers of cycles to failure: 3679 and 3900 cycles for the specimens of series A2%S3, and 8964 and 15000 cycles for the specimens of series A2%S3S5. Thus, on the average, series

A2%S3S5 sustained at least three times the number of cycles to failure resisted by series A2%S3. The difference between the two may be attributed to the presence of longer fibers in series A2%S3S5 (i.e. 50 mm versus 30 mm). However, the difference between the two series may also seem insignificant when the data are plotted on a log scale.

For the loading range of 10 to 70%, three specimens were tested for each series. Five out of the six specimens sustained more than 1.9×10^6 cycles, and one specimen of each series had not failed after 5×10^6 cycles. For these specimens, cyclic loading was stopped, and a monotonic loading test to failure was carried out. The corresponding MOR was larger than that of the control specimen (Table 2), confirming a previously noted result that prior cycling may lead to an improvement in strength.[3,10–12] The relatively large variability observed in the tests at this range of loading indicates the endurance limit of the material is probably being approached.

The maximum load as a percentage of the ultimate load is plotted versus the logarithm of the number of cycles to failure in Fig. 6 for all specimens, and a least-squares-fit line is derived. The corresponding *S–N* equation which can be used for prediction purposes is given by

$$S = 93 - 3.68 \log(N_f) \qquad (2)$$

where S is the maximum cyclic load as a percentage of the static MOR of the fiber-reinforced specimen, and N_f is the number of cycles to failure. The coefficient of correlation for the above equation is 0.976. It applies only to fiber-reinforced concrete with 2% hooked steel fibers as described in this study. Eqn (2) (Fig. 6) suggests an endurance limit of about 68% of ultimate load for 5×10^6 cycles.

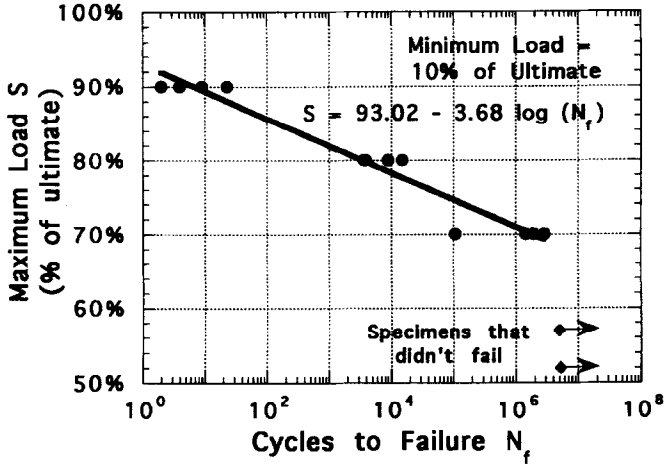

Fig. 6. Maximum applied load in percent versus number of cycles to failure.

Comparison with other investigations

Several prior investigations have dealt with fatigue in fiber-reinforced concrete.[9–13] An extensive investigation on the fatigue life of fiber-reinforced concrete was carried out by Ramakrishnan and coworkers.[10–12] Several particular aspects of their investigation are pointed out next because of differences with the present study: (1) the load ranges selected for the study were determined with respect to the reference plain concrete mix without fibers; (2) the frequency of cyclic loading was 20 Hz, a value considered too high to maintain an accurate load range and to minimize the effects of inertia; (3) the specimens were not precracked.

Ramakrishnan and coworkers concluded that for specimens reinforced with hooked-end steel fibers at volume fractions of 0.5 and 0.8% with aspect ratios of 75 and 100, the maximum absolute fatigue load under which the specimens could withstand 2×10^6 cycles without failure was 2.0 to 2.5 times that of corresponding specimens with a plain mix with no fibers. They also reported similar results for the absolute value of the fatigue load in specimens reinforced with hooked-end fibers with an aspect ratio of 100 at a volume fraction of 1%. Such optimistic results can be explained by the fact that the reference mix was taken as the concrete without fibers. In many cases, the presence of fibers leads to a significant increase in the MOR. Indeed, referring for instance to the results described in Refs 2 and 7, it can be observed that the average MOR of the control mix without fibers is 790 psi (5.45 MPa). On the other hand, the MOR of the same mix with 2% fibers (Table 1) exceeds 1265 psi (8.7 MPa) in all cases. In the present investigation, the reference MOR (or flexural strength) for adjusting fatigue load ranges for a given specimen was taken as that of the sister specimen of the same mix with fibers tested under static loading at the same age.

Wei *et al.*[13] also investigated the fatigue properties in bending of steel-fiber-reinforced

concrete. The main characteristics of the study include: (1) the fibers were flat fibers cut from low carbon steel sheets with an equivalent aspect ratio of about 60; (2) the fiber volume fraction ranged from 0 to 1.5%; (3) the frequency of cyclic loading ranged from 5 to 20 Hz; (4) the load range from minimum to maximum load was kept at 10% of ultimate; (5) the maximum load varied from 48 to 66% of ultimate; (6) fatigue loading was undertaken only to 1×10^6 cycles and fatigue damage was evaluated. Thus, it can be observed that such tests also dealt primarily with a conventional fiber-reinforced concrete (that is with a post-cracking strength possibly smaller than or equal to the cracking strength), that the frequency of loading was relatively high, thus inducing significant inertia effects during fatigue loading, and that it is likely that the specimens tested were not precracked. Hence the results of the study by Wei *et al.*[13] cannot be compared with those of this study. They are mentioned here for information only.

Hysteretic load versus deflection response

Hysteresis loops were recorded at various stages of the fatigue life of each specimen. Typical examples are shown in Figs 4, 7 and 8, and additional information can be found in Ref. 2. The area enclosed by the load versus deflection hysteresis loop describes the amount of damage done to the specimen during any recorded cycle. The hysteresis loop allows us to extract the values of deflections at P_{min} and P_{max} and

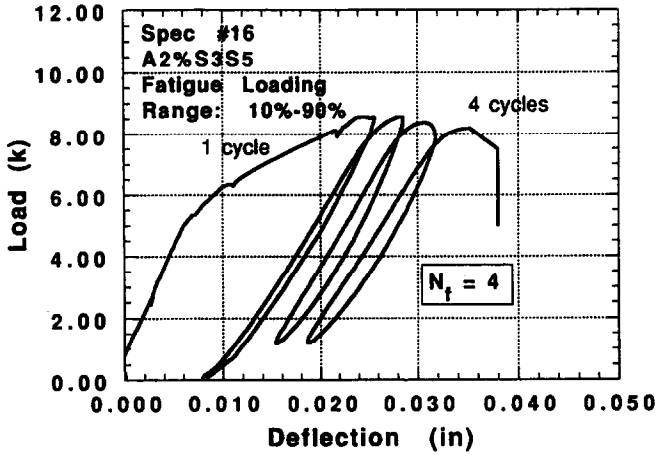

Fig. 7. Load versus deflection hysteretic response of specimen 16 under fatigue loading (1 kip = 4448 N; 1 in = 25 mm).

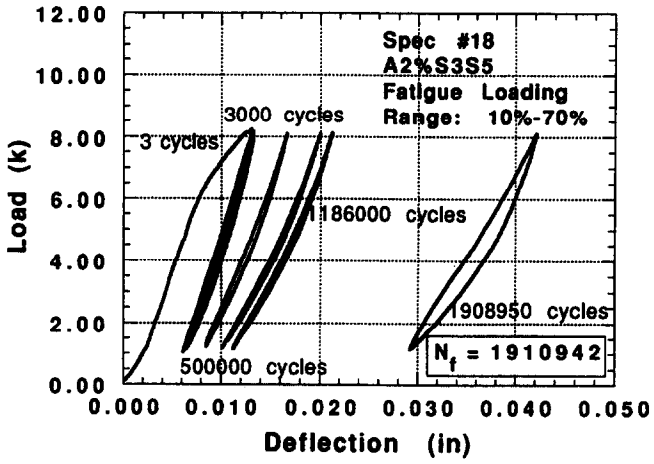

Fig. 8. Load versus deflection hysteretic response of specimen 18 under fatigue loading (1 kip = 4448 N; 1 in = 25 mm).

the permanent (non-recoverable) deflection at any cycle. Furthermore, the variation of the deflection between the minimum and maximum loads gives a good indication of the loss of stiffness of the specimen due to fatigue loading.

In the specimens subjected to the 10–90% loading range (Fig. 7), the material degradation is clearly illustrated by the large area enclosed by every loop and the resulting small number of cycles to failure. In the specimens subjected to the 10–80% and 10–70% loading ranges (Figs 4 and 8), the hysteresis loops had a larger area at the initial cycles, followed by a stabilization period during which the loops remained almost constant; then, closer to the fatigue life of the specimen, the area enclosed by the hysteresis loop increased again. Generally, a relatively large permanent (non-recoverable) deflection developed under cyclic loading

Another important result of the fatigue tests is the increase in the differential deflection $\Delta\delta$ between the minimum and maximum applied load levels (P_{min} and P_{max}) with the number of loading cycles. Typical results are illustrated in Figs 9 and 10.

Specimens that survived 5×10^6 cycles

The two specimens that did not fail under fatigue loading, specimens 9 (A2%S3) and 17 (A2%S3S5), showed different behaviors. Specimen 9 showed a period of constant permanent deformation until about 2×10^6 cycles, after which there was a substantial increase in the permanent deformation until about 3×10^6

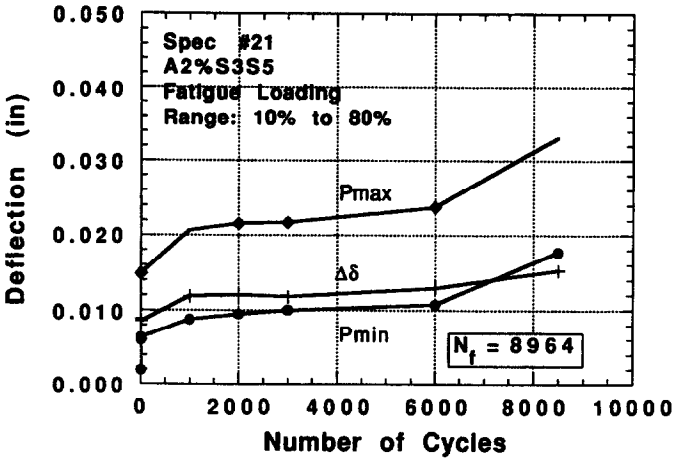

Fig. 9. Variation of deflection with applied number of cycles for specimen 21 (1 kip = 4448 N).

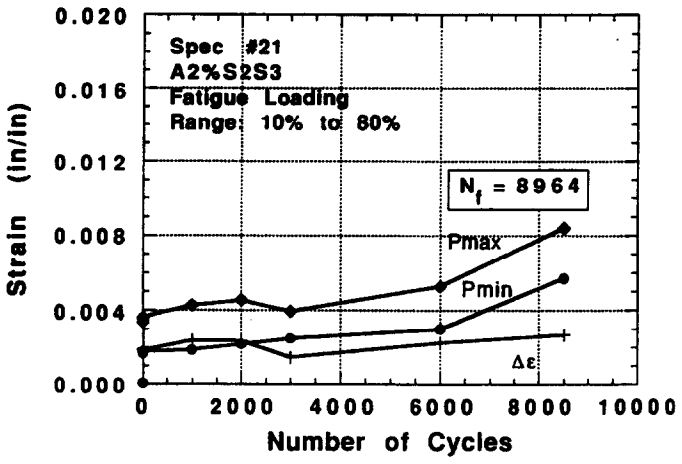

Fig. 11. Variation of extreme fiber tensile strain with applied number of cycles for specimen 21 (1 in in^{-1} = 1 mm mm^{-1}).

cycles, followed by another period of constant increase until the fatigue tests were interrupted at 5.276×10^6 cycles. Specimen 17 showed a period of constant permanent deformation until the interruption of the fatigue test at 5×10^6 cycles. The post-fatigue static load versus deflection curves of specimens 9 and 17 were determined (Table 2). As observed in previous investigations, the MOR obtained after fatigue loading was higher than that before fatigue loading, here considered to be the control.

Load versus tensile strain capacity

The average tensile strain in the constant moment region is related to the average crack width observed. This is because the elastic tensile strains, being of the order of 2×10^4, can be neglected. Most specimens had one to three visible cracks along the constant moment region.

Typical variations of the average tensile strain in the constant moment region at the minimum and maximum applied load levels (P_{min} and P_{max}) and the tensile strain difference $\Delta\varepsilon$ between the minimum and maximum loads are plotted against the number of cycles in Figs 11 and 12 for two specimens that failed under fatigue loading. A trend similar to what was observed for deflection is noted; namely, a larger rate of increase in the early cycles, followed by a period of stabilization with a constant rate of increase up to about 90 to 95% of

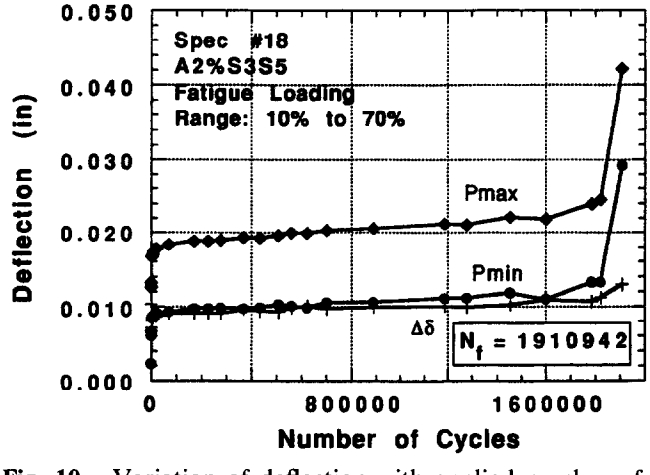

Fig. 10. Variation of deflection with applied number of cycles for specimen 18 (1 in = 25 mm).

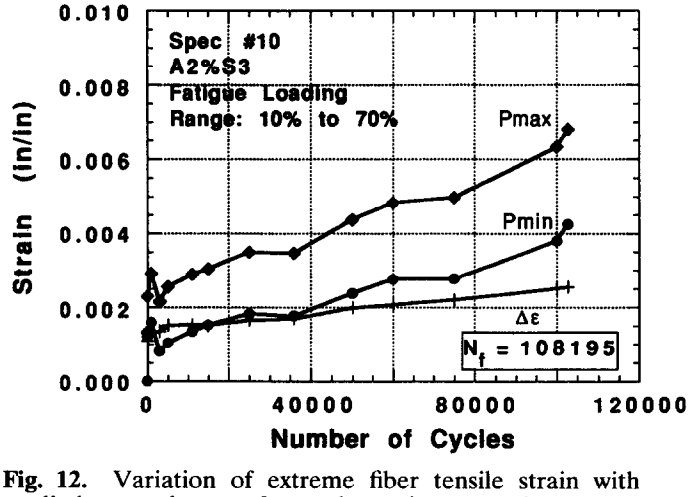

Fig. 12. Variation of extreme fiber tensile strain with applied number of cycles for specimen 10 (1 in in^{-1} = 1 mm mm^{-1}).

fatigue life, then again a higher rate of increase leading to failure.

CONCLUSIONS

1. Specimens reinforced with hooked-end steel fibers at volume fractions of 2% showed average fatigue lives of the order of 10 cycles for loads ranging between 10 and 90% of their static strength, 8000 cycles for loads ranging between 10 and 80%, and more than 2.7×10^6 cycles for loads ranging between 10 and 70%. These values hold, assuming the specimens are pre-cracked. Substantially larger values can be achieved with uncracked specimens.
2. From the limited number of tests undertaken in this study, the derived S–N curve in bending of HESFRC with 2 vol% of hooked steel fibers is given by (Fig. 2) $S = 93 - 3.68 \log(N_f)$, where S is the maximum cyclic load as a percentage of the static MOR of the fiber-reinforced specimen, and N_f is the number of cycles to failure. The coefficient of correlation for the above equation is 0.976. It can be inferred that the fatigue life of fiber-reinforced concrete mixtures containing 2 vol% of hooked steel fibers is of the order of 68% of their static flexural strength for 5×10^6 cycles, 67% for 1×10^7 cycles, and 65% for 5×10^7 cycles. For all practical purposes, a stress range of 65% can be taken as the endurance limit in design.
3. Concrete mixtures reinforced with 2 vol% hooked-end steel fibers, with aspect ratios of either 60 or an equal mix of 60 and 100, showed essentially similar behavior under fatigue loading. This may imply that the influence of aspect ratio on fatigue life is not as significant as the volume fraction of fibers; however, a more realistic explanation is that, with hooked fibers, the fiber pull-out resistance after debonding is primarily controlled by the end hook and not by the fiber length.
4. Fiber-reinforced concrete mixtures containing 2 vol% of hooked steel fibers can sustain cyclic fatigue stresses (in absolute values) more than twice those of plain concrete (control) without fibers.
5. An attempt was made to establish a correlation between E_{dyn} and MOR for static loading, with the hope of extending the correlation for fatigue loading. Results of this investigation showed that there is little correlation between a high value of dynamic modulus and a high fatigue life.

The main recommendation that results from this study is that, for mixes with 2 vol% hooked steel fibers, a safe endurance limit for cyclic fatigue loading in bending can be taken at about 65% of the static ultimate strength (or equivalently the MOR) obtained from a control specimen with fibers. This result should be valid even if the beam is cracked at maximum load.

ACKNOWLEDGEMENTS

The research described herein was supported by the Strategic Highway Research Program (SHRP). The overall research work was undertaken by a consortium of three universities, namely: North Carolina State University (prime contractor) with P. Zia (project director), S. Ahmad, and M. Lemming; University of Michigan with A.E. Naaman (principal investigator); University of Arkansas with R.P. Elliot and J.J. Schemmel. The research team received valuable support, counsel, and guidance from the Expert Task Group. The support and encouragement provided by Inam Jawed, SHRP program manager, is deeply appreciated. Opinions expressed in this paper are those of the authors and do not necessarily reflect the views of SHRP.

REFERENCES

1. Zia, P., Ahmad, S., Lemming, M., Elliott, R. P. & Shemmel, J. J., Mechanical properties of high performance concretes, Vols 1–5 and 7, SHRP — Strategic Highway Research Program, National Research Council, Report Nos SHRP-C 361–365 and 367, Washington, DC, 1993.
2. Naaman, A. E., Alkhairi, F. M. & Hammoud, H., Mechanical behavior of high performance concrete, Vol. 6: high early strength fiber reinforced concrete, Strategic Highway Research Program, Report No. SHRP-C-366, National Research Council, Washington, DC, 1993.
3. Naaman, A. E. & Harajli, M. H., *Mechanical Properties of High Performance Fiber Concretes: A State-of-the-Art Report* (SHRP-C/WP-90-004), SHRP National Research Council, Washington DC, 1990.
4. Alkhairi, F. M. & Naaman, A. E., *An Annotated Bibliography on High Strength Fiber Reinforced Concrete*, Department of Civil Engineering, University of Michigan, Report No. UMCE 91-08, December, 1991.
5. Reinhardt, H. W. & Naaman, A. E., *High Performance Fiber Reinforced Cement Composites*, RILEM Proceedings 15, Chapman and Hall, London, 1992.
6. Naaman, A. E. & Alkhairi, F. M., Compression properties of high early strength fiber reinforced concrete, in N. Banthia & S. Mindess (eds), *Fiber*

Reinforced Concrete — Modern Developments (Workshop Proceedings, Toronto), The University of British Columbia, Vancouver, Canada, March, 1995, pp. 129–46.
7. Naaman, A. E. & Alkhairi, F. M., Bending properties of high early strength fiber reinforced concrete — HESFRC, *Proceedings NSF–ACI International Workshop on High Performance Concrete*, Bangkok, Thailand, November, 1994, pp. 24.1–23.
8. Ramakrishnan, V., Meyer, C., Naaman, A. E., Zhao, G. & Fang, L., Cyclic behavior, fatigue strength, endurance limit and models for fatigue behavior of FRC, in A. E. Naaman & H. W. Reinhardt (eds), *High Performance Fiber Reinforced Cement Composites — HPFRCC 2*, RILEM publication 31, E&FN Spon, London, 1996, Chapter 4.
9. Batson, G., Ball, C., Bailey, L., Landers, C. & Hooks, J., Flexural fatigue strength of steel fiber reinforced concrete beams. *ACI Journal*, **69**(11) (1972) 673–677.
10. Ramakrishnan, V., Oberling, G. & Tatnall, P., *Flexural Fatigue Strength of Steel Fiber Reinforced Concrete in Fiber Reinforced Concrete: Properties and Applications*, SP 105-13, American Concrete Institute, Detroit, 1987, pp. 225–45.
11. Ramakrishnan, V., Wu, G. Y. & Hosalli, G., Flexural fatigue strength, endurance limit, and impact strength of fiber reinforced concretes, paper presented at *68th Annual Meeting of the Transportation Research Board*, Washington, DC, 1989.
12. Ramakrishnan, V. & Lokvik, B. J., in H. W. Reinhardt & A. E. Naaman (eds), *Flexural Fatigue Strength of Fiber Reinforced Concretes High Performance Fiber Reinforced Cement Composites*, RILEM Proceedings 15, Chapman and Hall, London, 1992.
13. Wei, S., Jianming, G. & Yun, Y., Study of the fatigue performance and damage mechanisms of fiber reinforced concrete. *ACI Mater. J.*, **93**(3) (1996) 206–211.